Semiconductor Sensors:

Ch6: Gas Sensors cont.

Work Function Effect Gas Sensors

Lecturer: Dr. Navid Alaei-Sheini
Assistant Professor of Electrical Enginnering
Shahid Chamran University of Ahvaz

جذب فیزیکی و شیمیایی به سطح

Fig. 3 Gas adsorption on a solid: physisorption (*left*) and chemisorption (*right*)

Fleischer, M., & Lehmann, M. (Eds.). (2012). Solid State Gas Sensors-Industrial Application (Vol. 11). Springer Science & Business Media.

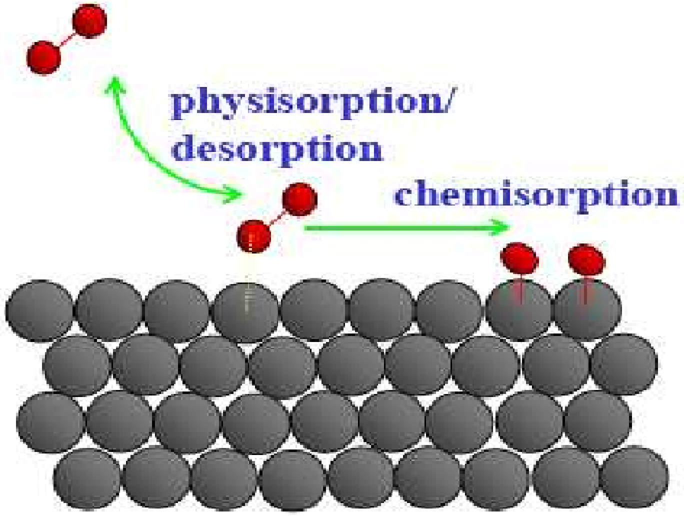

Griffiths, Hannah. Layered double hydroxides: structure, synthesis and catalytic applications. Diss. University of Huddersfield, 2012.

جذب فیزیکی و شیمیایی به سطح

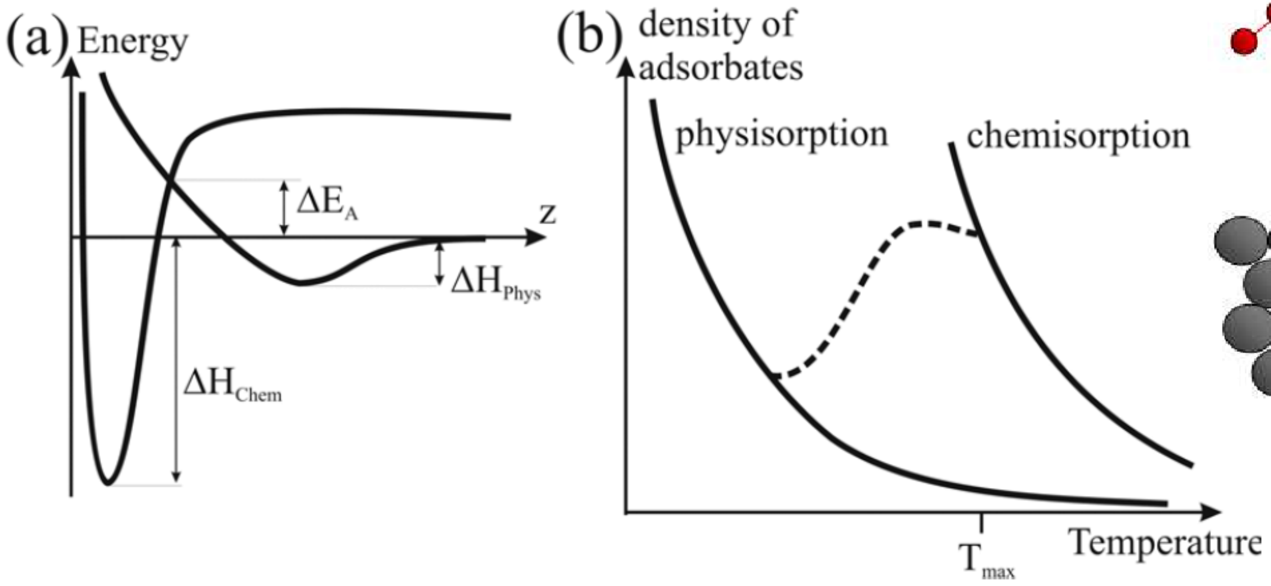

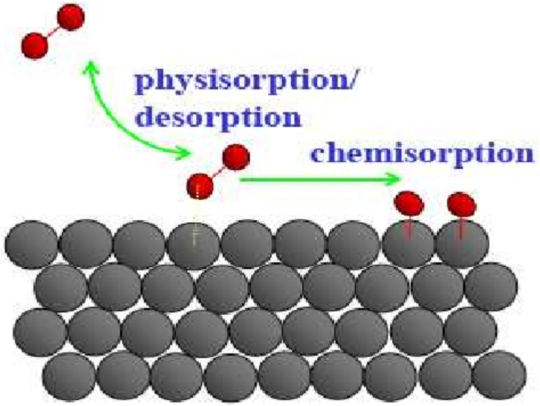

(a) Lenard-Jones model for physisorption and chemisorption of molecules. Typical adsorption isobars are shown in (b). The solid lines are equilibrium physisorption and chemisorption isobars, the dashed line represents irreversible chemisorption. A maximum coverage of chemisorbed molecules is obtained at T_{max} .

ΔE_A is the activation barrier for chemisorption and ΔH_{chemis} the heat of chemisorption. Under steady state conditions

Batzill, Matthias. "Surface science studies of gas sensing materials: SnO2." *Sensors* (2006)

جذب شیمیایی به سطح

In case of dissociative chemisorption, the molecular coverage **Θ**x is calculated from a simple rate equation, as displayed in Fig. 4.

$$\frac{d\Theta_X}{dt} = 2p_X k_a (1-\Theta_X)^2 - 2k_d \Theta_X^2$$

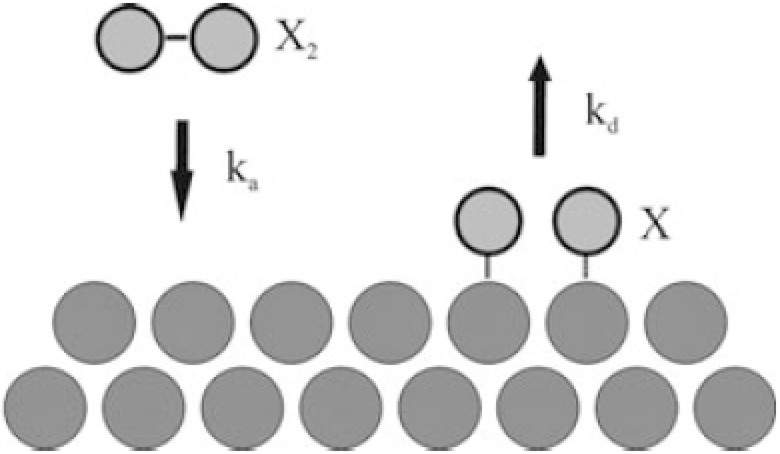

Fig. 4 Rate equation (*left*) and schematic view of dissociative adsorption and desorption (*right*)

p_X is the partial pressure; $k_{a/d}$ are rate constants for adsorption and desorption.

Fleischer, M., & Lehmann, M. (Eds.). (2012). Solid State Gas Sensors-Industrial Application (Vol. 11). Springer Science & Business Media.

جذب شیمیایی به سطح

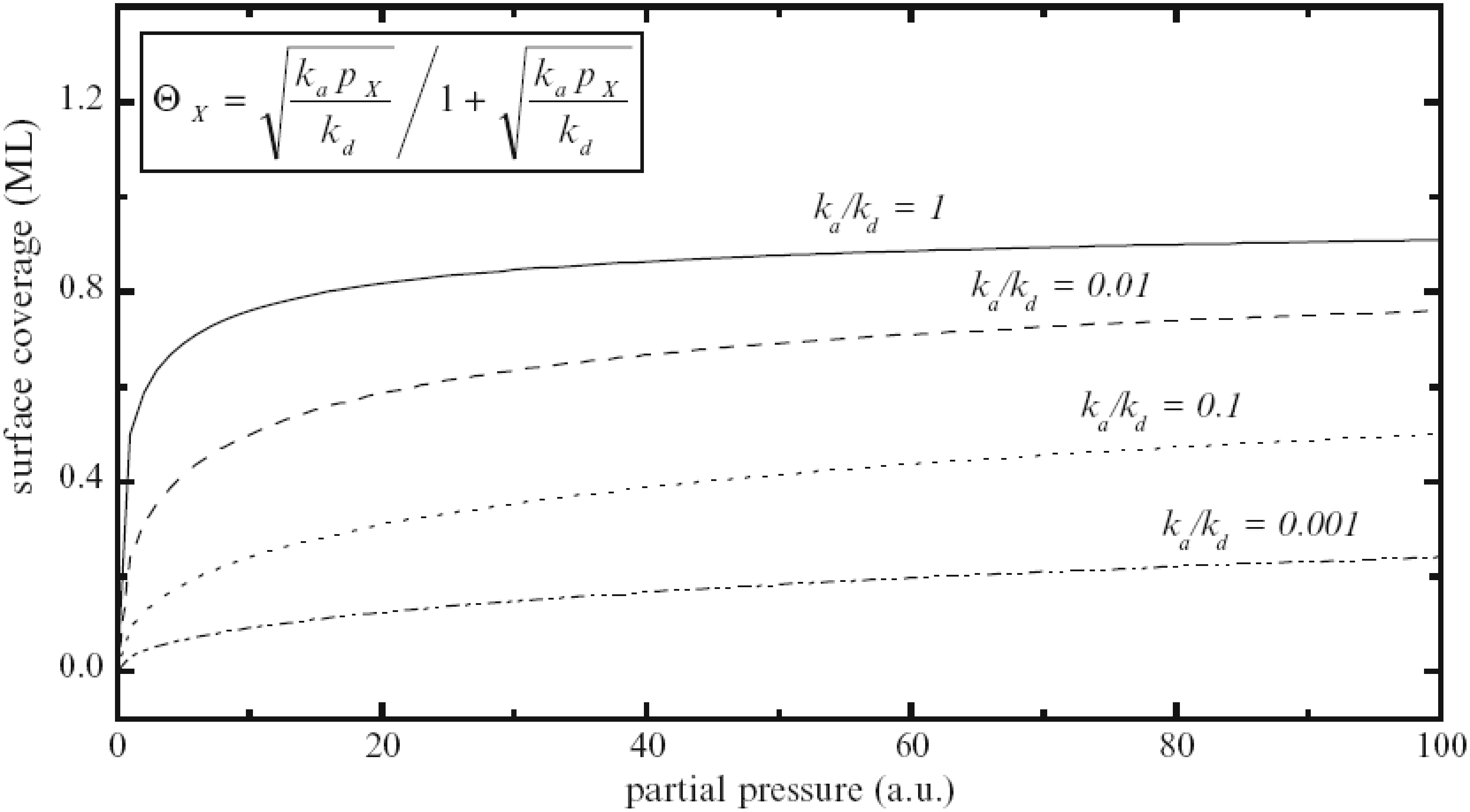

Fig. 5 Surface coverage equation (*inset*) and graphical solution of dissociative adsorption and desorption with respect to partial pressure

Fleischer, M., & Lehmann, M. (Eds.). (2012). Solid State Gas Sensors-Industrial Application (Vol. 11). Springer Science & Business Media.

Work Function for various elements (eV)

تابع کار مواد مختلف

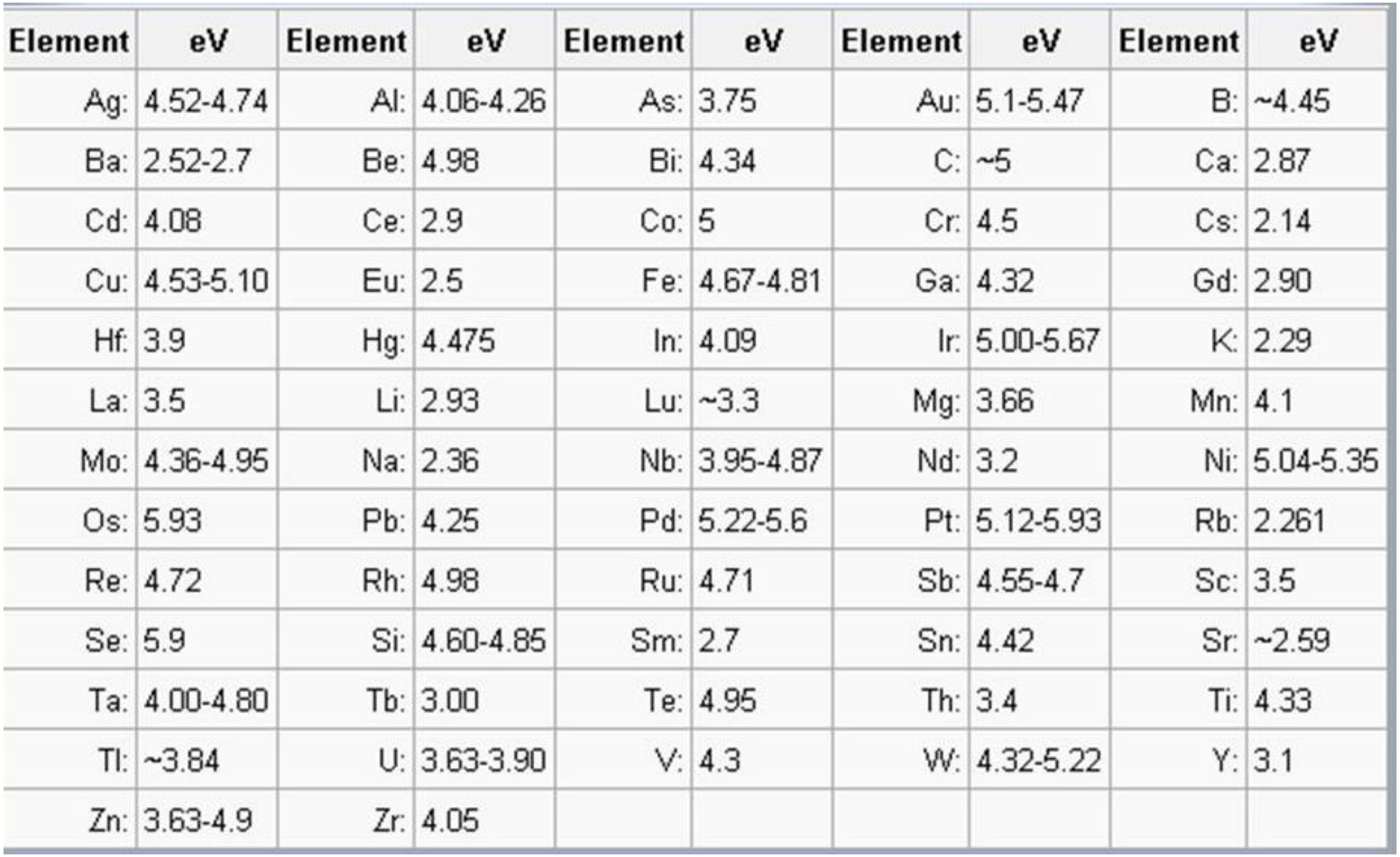

Element	eV	Element	eV	Element	eV	Element	eV	Element	eV
Ag:	4.52-4.74	Al:	4.06-4.26	As:	3.75	Au:	5.1-5.47	B:	~4.45
Ba:	2.52-2.7	Be:	4.98	Bi:	4.34	C:	~5	Ca:	2.87
Cd:	4.08	Ce:	2.9	Co:	5	Cr:	4.5	Cs:	2.14
Cu:	4.53-5.10	Eu:	2.5	Fe:	4.67-4.81	Ga:	4.32	Gd:	2.90
Hf:	3.9	Hg:	4.475	In:	4.09	Ir:	5.00-5.67	K:	2.29
La:	3.5	Li:	2.93	Lu:	~3.3	Mg:	3.66	Mn:	4.1
Mo:	4.36-4.95	Na:	2.36	Nb:	3.95-4.87	Nd:	3.2	Ni:	5.04-5.35
Os:	5.93	Pb:	4.25	Pd:	5.22-5.6	Pt:	5.12-5.93	Rb:	2.261
Re:	4.72	Rh:	4.98	Ru:	4.71	Sb:	4.55-4.7	Sc:	3.5
Se:	5.9	Si:	4.60-4.85	Sm:	2.7	Sn:	4.42	Sr:	~2.59
Ta:	4.00-4.80	Tb:	3.00	Te:	4.95	Th:	3.4	Ti:	4.33
Tl:	~3.84	U:	3.63-3.90	V:	4.3	W:	4.32-5.22	Y:	3.1
Zn:	3.63-4.9	Zr:	4.05						

The work function is defined as the minimum energy, which is necessary to extract an electron from a neutral solid.

Presentation on theme: "Electrons in Atoms and Periodic Properties", by :Jocelyn Blind. 6

وابستگی تابع کار فلزات به صفحه کریستالی

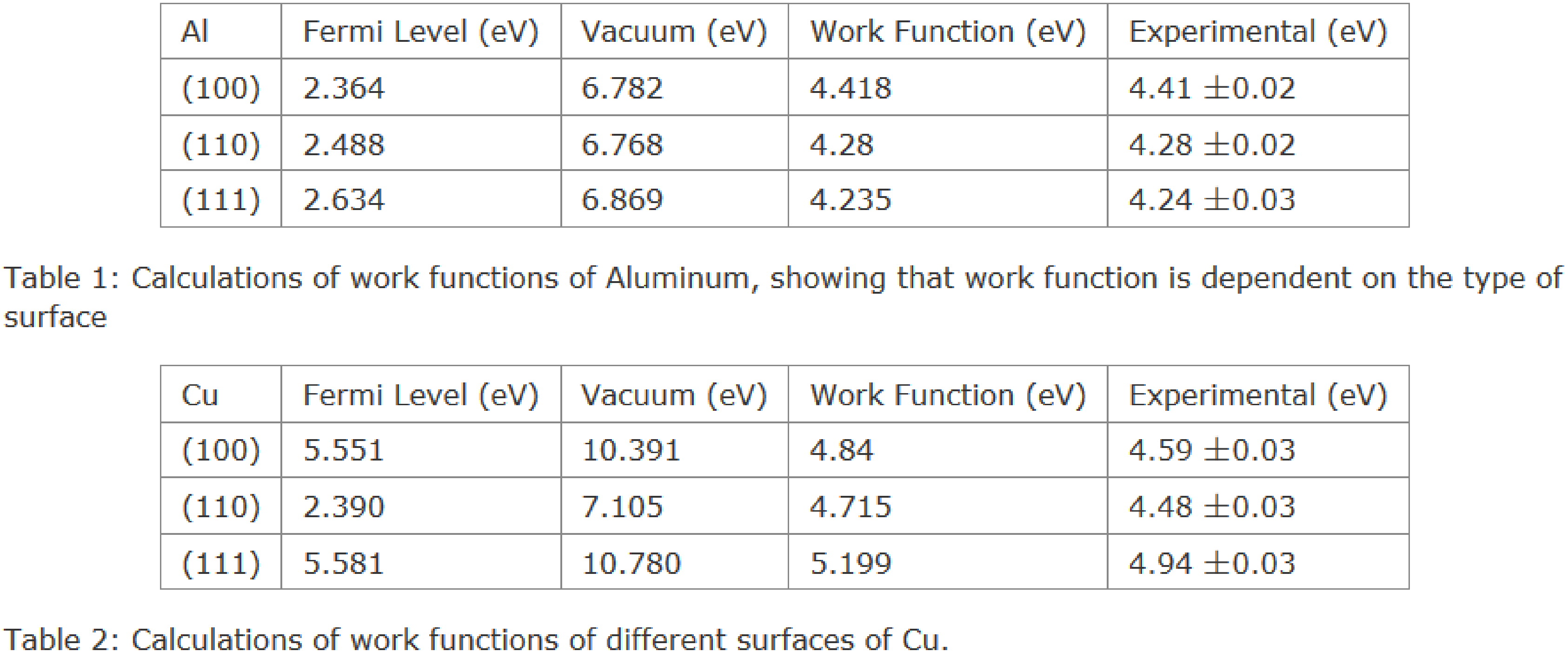

Al	Fermi Level (eV)	Vacuum (eV)	Work Function (eV)	Experimental (eV)
(100)	2.364	6.782	4.418	4.41 ±0.02
(110)	2.488	6.768	4.28	4.28 ±0.02
(111)	2.634	6.869	4.235	4.24 ±0.03

Table 1: Calculations of work functions of Aluminum, showing that work function is dependent on the type of surface

Cu	Fermi Level (eV)	Vacuum (eV)	Work Function (eV)	Experimental (eV)
(100)	5.551	10.391	4.84	4.59 ±0.03
(110)	2.390	7.105	4.715	4.48 ±0.03
(111)	5.581	10.780	5.199	4.94 ±0.03

Table 2: Calculations of work functions of different surfaces of Cu.

اثر تغییر در تابع کار با جذب گاز به سطح

Work Function Change Caused by Gas Adsorption

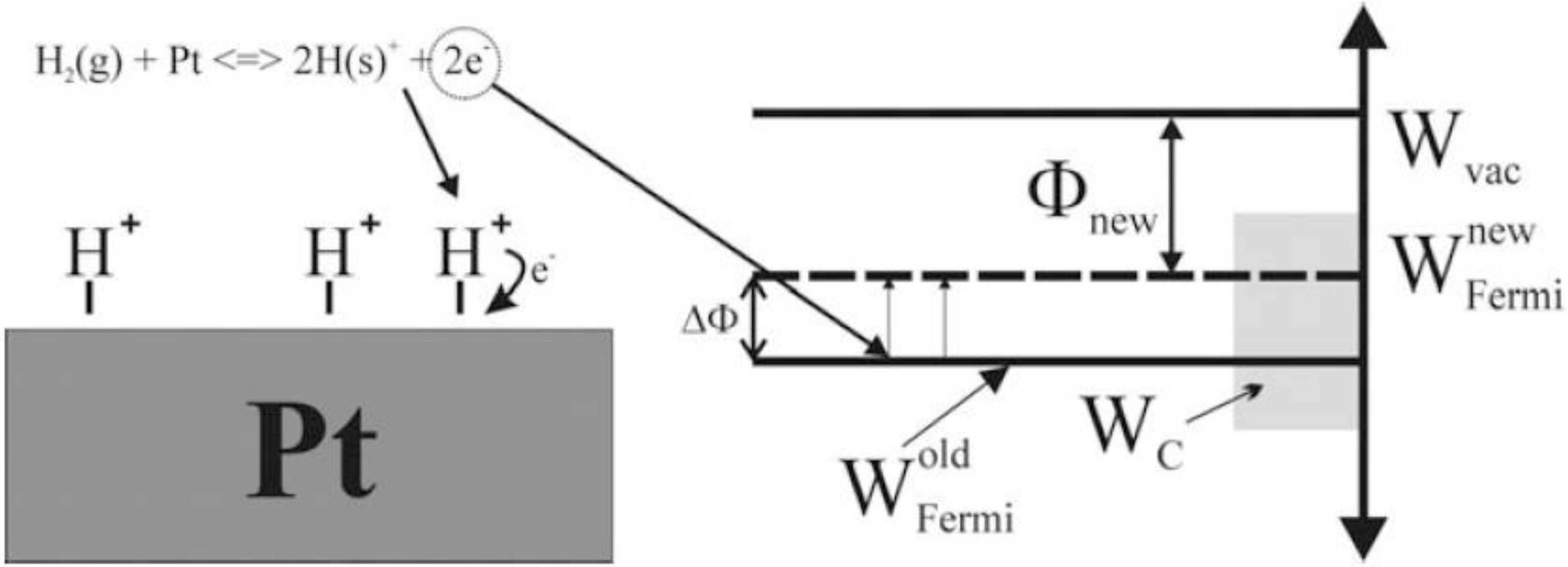

Fig. 7 Work function change caused by chemisorption of hydrogen on clean platinum

Fleischer, M., & Lehmann, M. (Eds.). (2012). Solid State Gas Sensors-Industrial Application (Vol. 11). Springer Science & Business Media.

وابستگی تغییر تابع کار گیت پلاتینی به غلظت هیدروژن

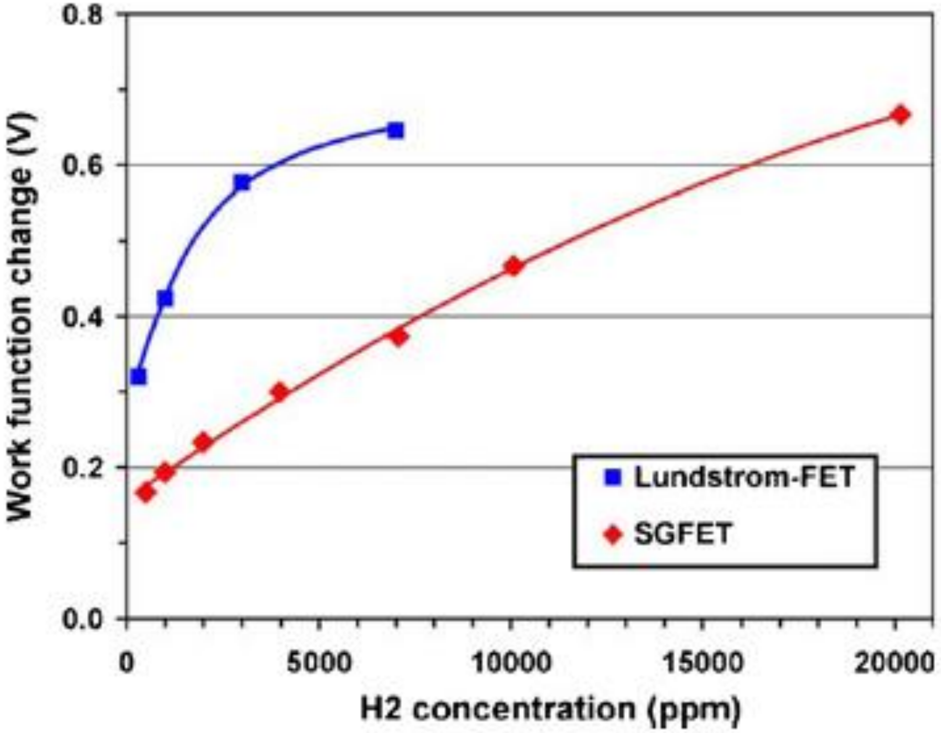

Fig. 36. Hydrogen sensitivity of Lundstrom-FET and SG-FET with Pt gate at low H_2 concentrations. From [98].

A. Oprea., N Bârsan,., &U. Weimar, Work function changes in gas sensitive materials: Fundamentals and applications. *Sensors and Actuators B: Chemical*, (2009).

حسگر گاز شاتکی

اثر: تغییر تابع کار فلز و ارتفاع سطح شاتکی با گاز.

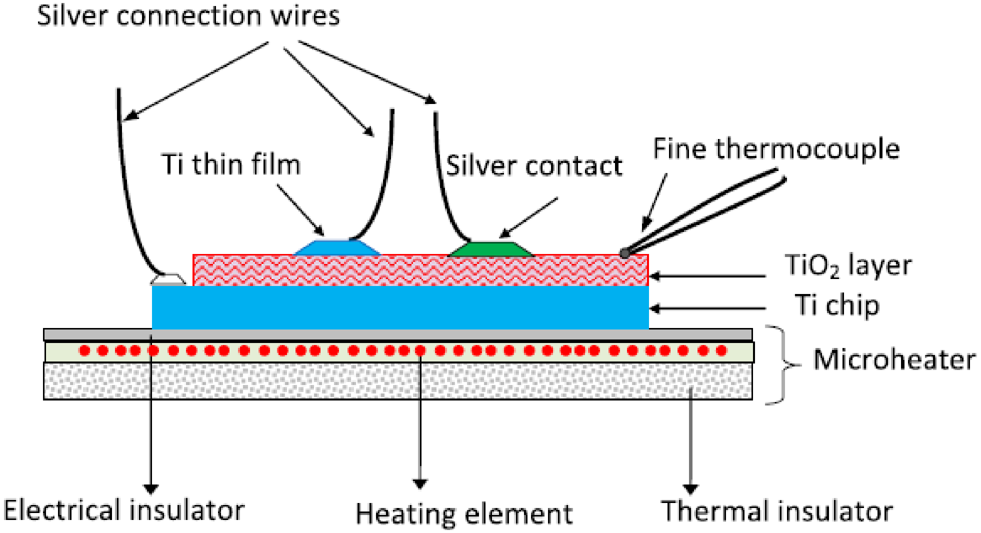

The schematic diagram of the Ti–TiO2 and Ag–TiO2 junctions fabricated on a thermally oxidized titanium metal chip mounted on a microheater.

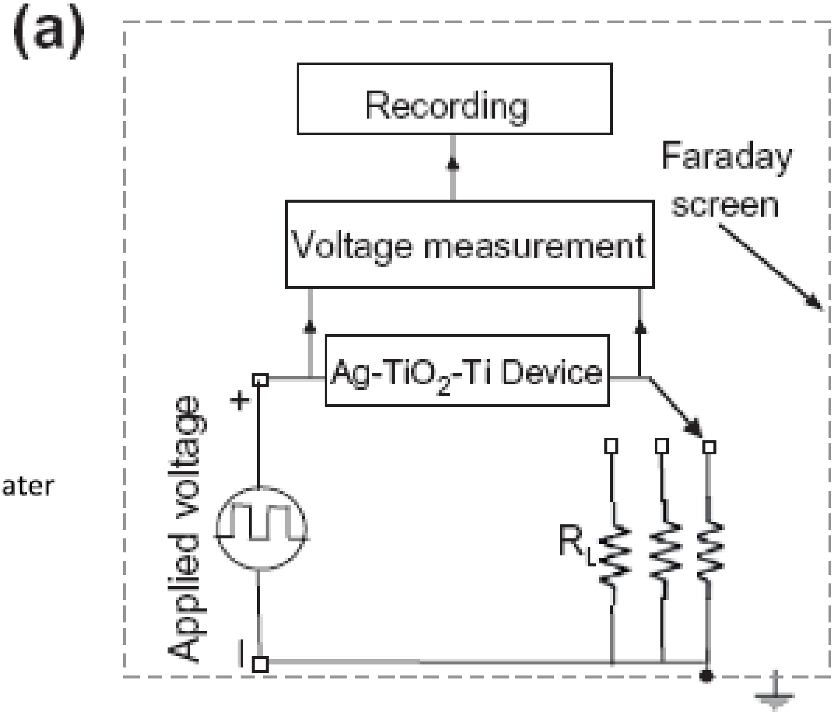

The experimental setup used for the measurement of the I–V characteristics of the forward biased Ag–TiO2 diode

F. Hossein-Babaei and S. Rahbarpour “Titanium and silver contacts on thermally oxidized titanium ch
Electrical and gas sensing properties”, Solid State Electronics, 2011.

حسگر گاز شاتکی

اثر: تغییر تابع کار فلز و ارتفاع سطح شاتکی با گاز.

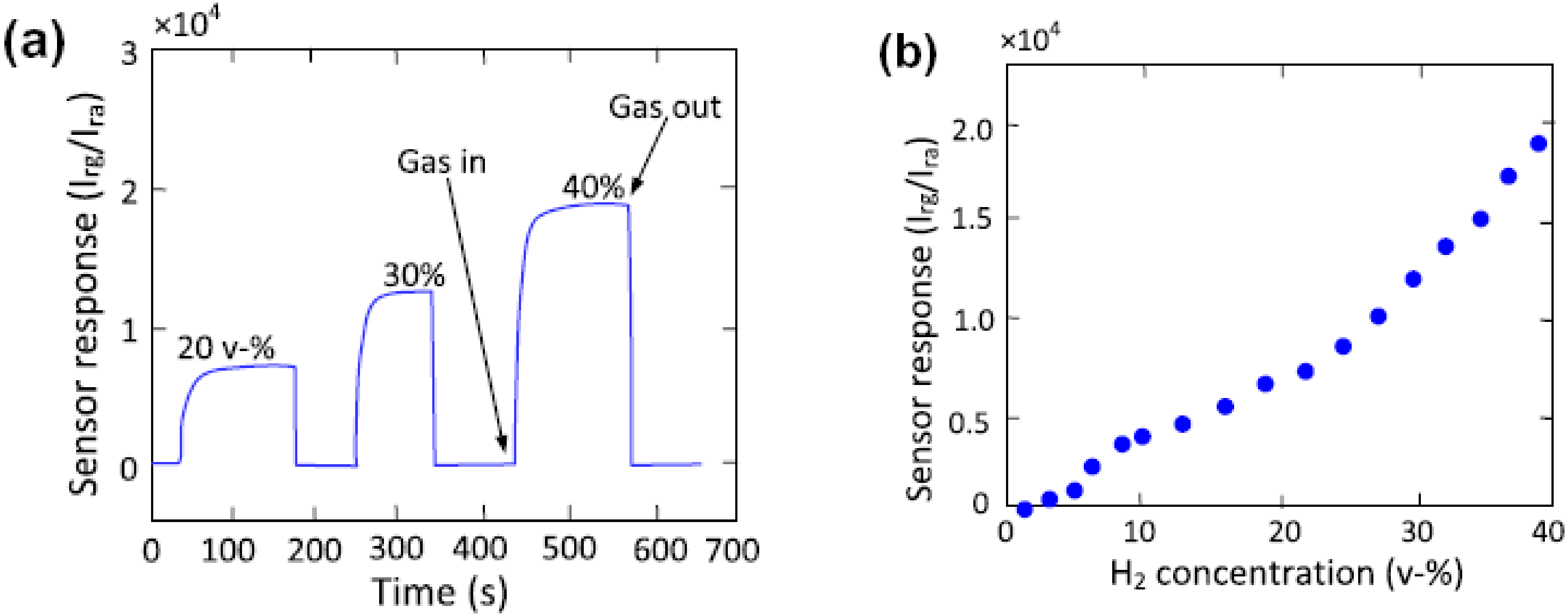

Fig. 7. The transient (a) and the steady state (b) responses of the Ag–TiO_2 sensor operating at 300 °C to different concentration levels of H_2 in air.

where I_{rg} and I_{ra} are the reverse currents measured at the contaminated air and clean air, respectively.

F. Hossein-Babaei and S. Rahbarpour “Titanium and silver contacts on thermally oxidized titanium ch
Electrical and gas sensing properties”, Solid State Electronics, 2011.

حسگر گاز شاتکی

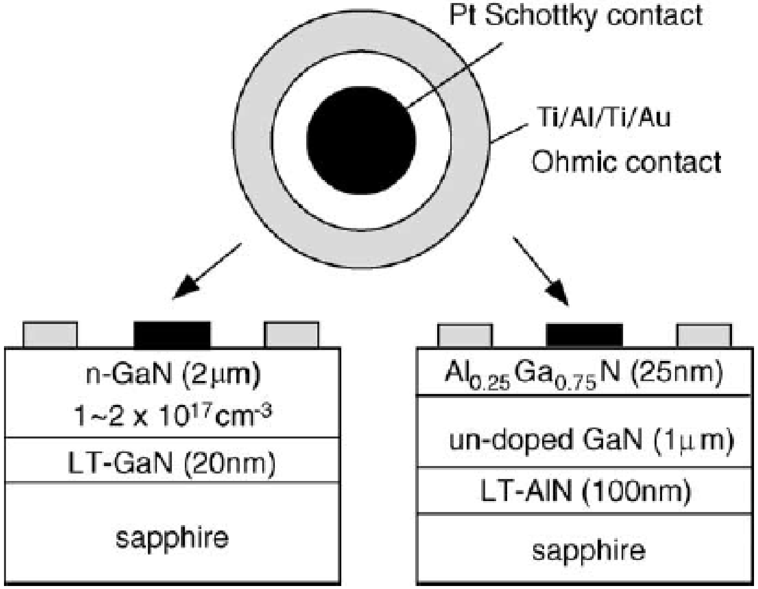

Fig. 1. Structures of Pt/GaN and Pt/AlGaN/GaN Schottky diodes used in this study.

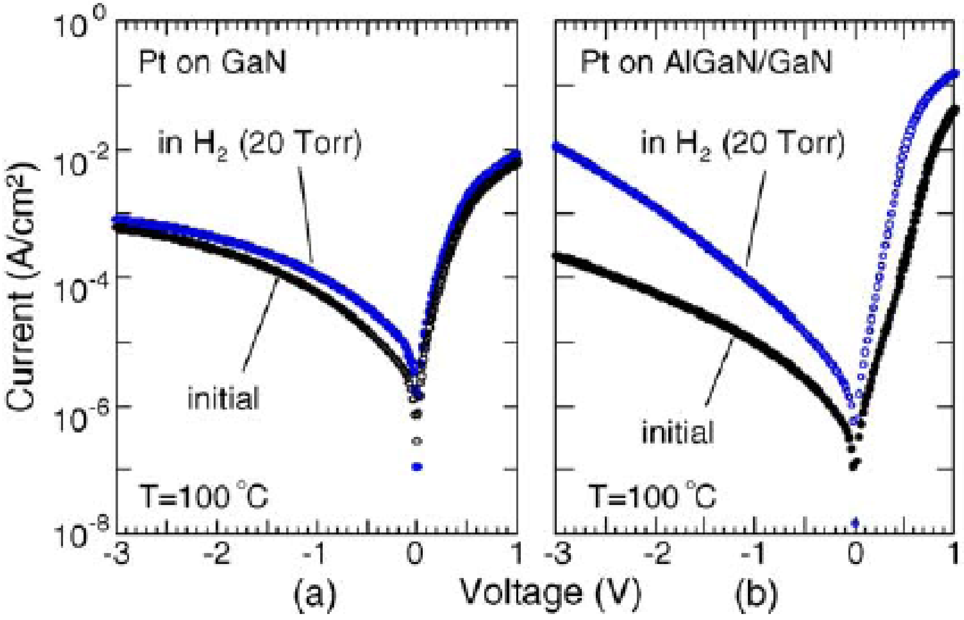

Fig. 2. Typical *I*–*V* characteristics of (a) Pt/GaN and (b) Pt/AlGaN/GaN Schottky diodes before and after exposure to H_2 at 100 °C.

K. Matsuo et al. “Pt Schottky diode gas sensors formed on GaN and AlGaN/GaN heterostructure”, Applied surface sciences, 2006.

حسگر گاز شاتکی

Observed current changes are due to changes in Schottky barrier heights (SBH). Such a change of SBH can be either due to H-induced formation of interfacial dipole, or to hydrogen passivation of interface states causing Fermi level pinning at the Schottky interface.

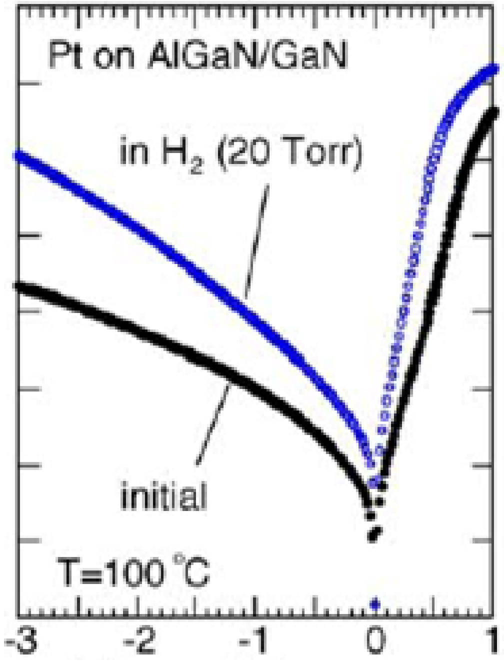

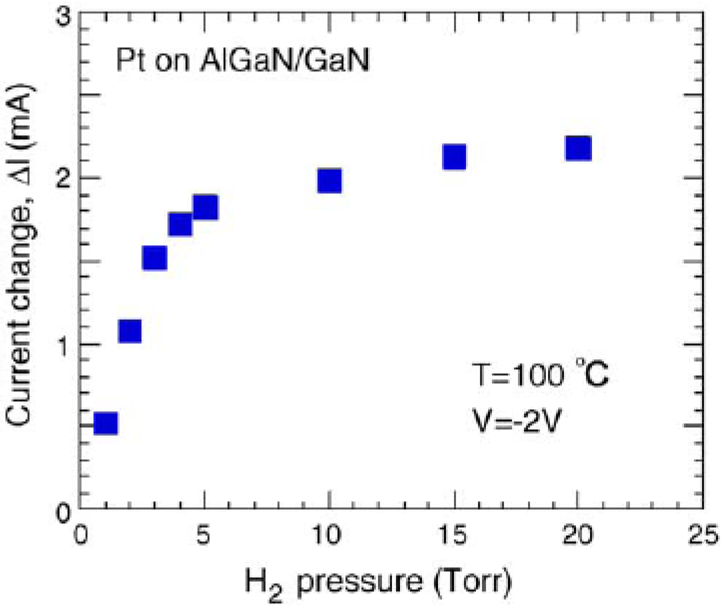

Fig. 3. Current change, ΔI, at $V = -2$ V at 100 °C as a function of H_2 pressure for a Pt/AlGaN/GaN Schottky diode.

K. Matsuo et al. “Pt Schottky diode gas sensors formed on GaN and AlGaN/GaN heterostructure”, Applied surface sciences, 2006.

سطح در ساختارهای کربنی

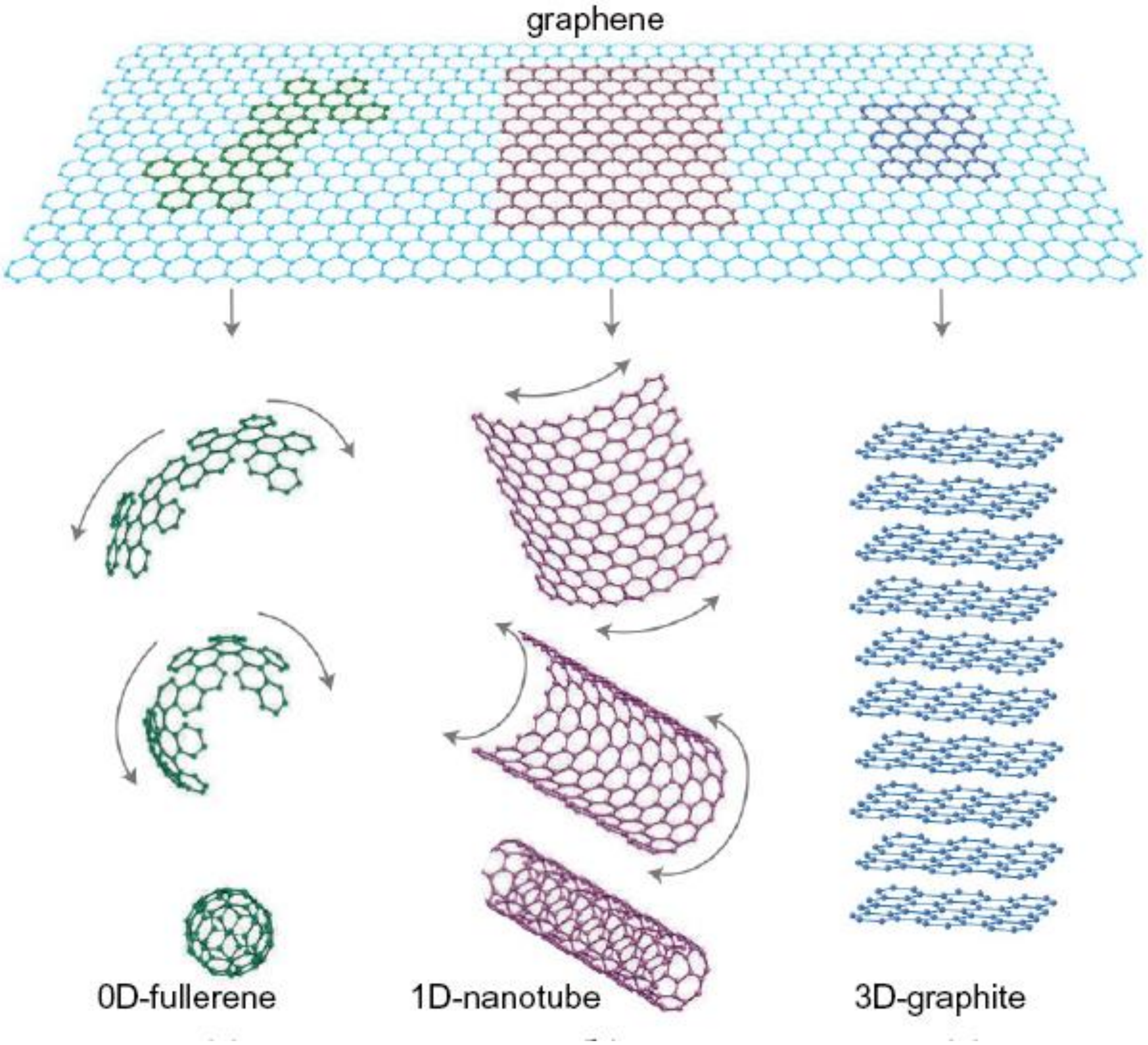

D'Souza, Francis, and Karl M. Kadish, eds. *Handbook of carbon nano materials*. World Scientific Publishing Company, 2011.

حسگرهای با ساختار کربنی

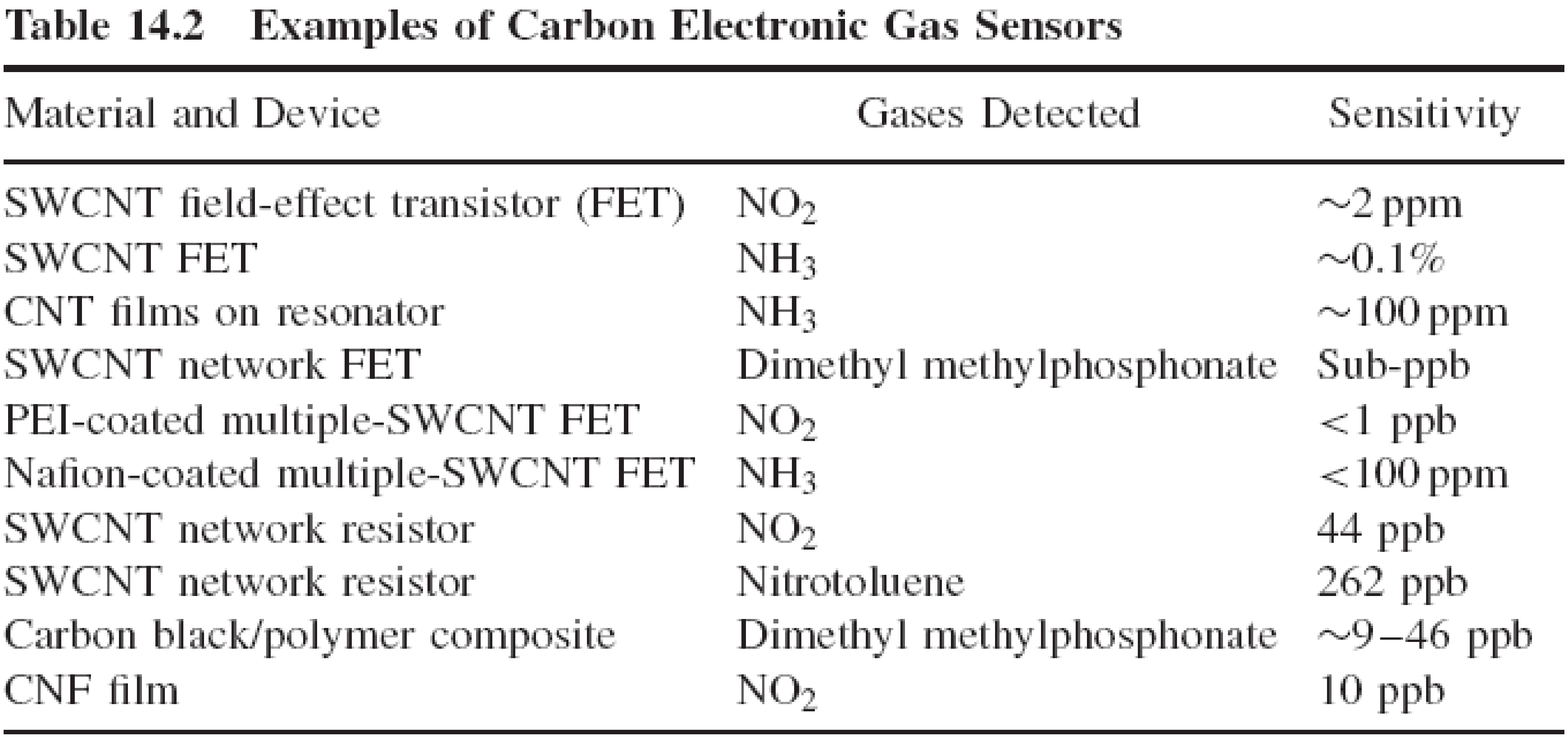

Table 14.2 Examples of Carbon Electronic Gas Sensors

Material and Device	Gases Detected	Sensitivity
SWCNT field-effect transistor (FET)	NO_2	~2 ppm
SWCNT FET	NH_3	~0.1%
CNT films on resonator	NH_3	~100 ppm
SWCNT network FET	Dimethyl methylphosphonate	Sub-ppb
PEI-coated multiple-SWCNT FET	NO_2	<1 ppb
Nafion-coated multiple-SWCNT FET	NH_3	<100 ppm
SWCNT network resistor	NO_2	44 ppb
SWCNT network resistor	Nitrotoluene	262 ppb
Carbon black/polymer composite	Dimethyl methylphosphonate	~9–46 ppb
CNF film	NO_2	10 ppb

SWCNT: Single-Walled Carbon Nano Tube

P. Serp and J. L. Figueiredo, eds. *Carbon materials for catalysis*. John Wiley & Sons, 2009.

آنالیز EDAX در ساختار کربنی برای مشخص کردن درصد جذب اکسیژن

EDAX: Energy dispersive X-ray spectroscopy

Table I: Carbon and Oxygen concentration (%) determined from EDAX studies.

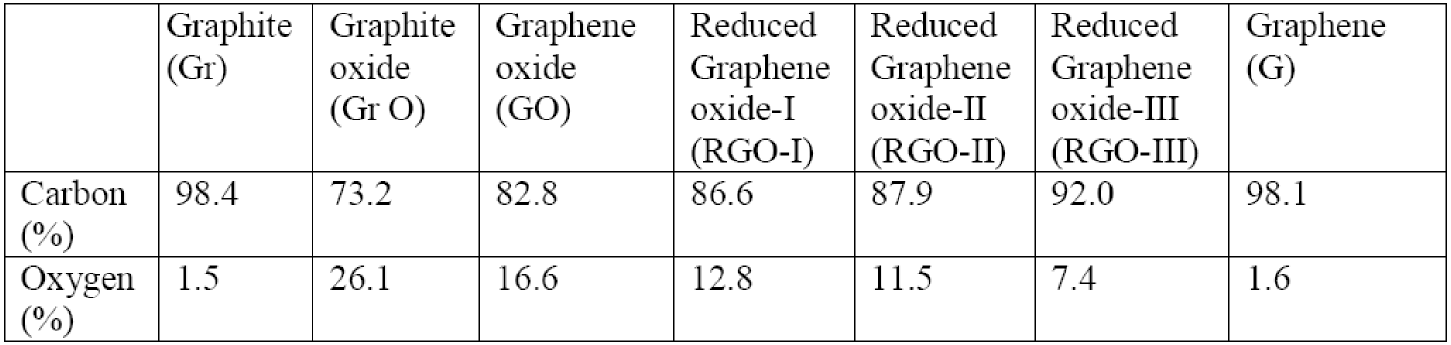

	Graphite (Gr)	Graphite oxide (Gr O)	Graphene oxide (GO)	Reduced Graphene oxide-I (RGO-I)	Reduced Graphene oxide-II (RGO-II)	Reduced Graphene oxide-III (RGO-III)	Graphene (G)
Carbon (%)	98.4	73.2	82.8	86.6	87.9	92.0	98.1
Oxygen (%)	1.5	26.1	16.6	12.8	11.5	7.4	1.6

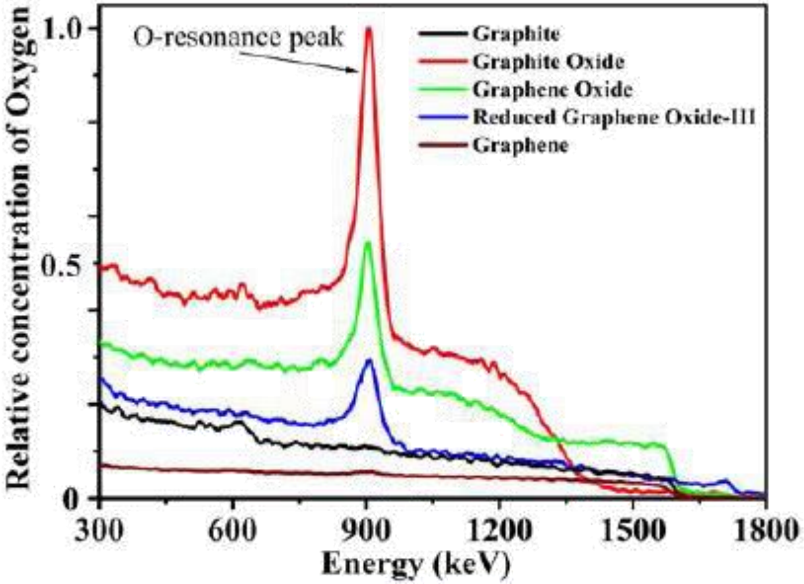

Mishra, Mukesh, et al. "Role of oxygen in the work function modification at various stages of chemically synthesized graphene." *The Journal of Physical Chemistry C* (2013).

اثر جذب اکسیژن به سطح گرافن:

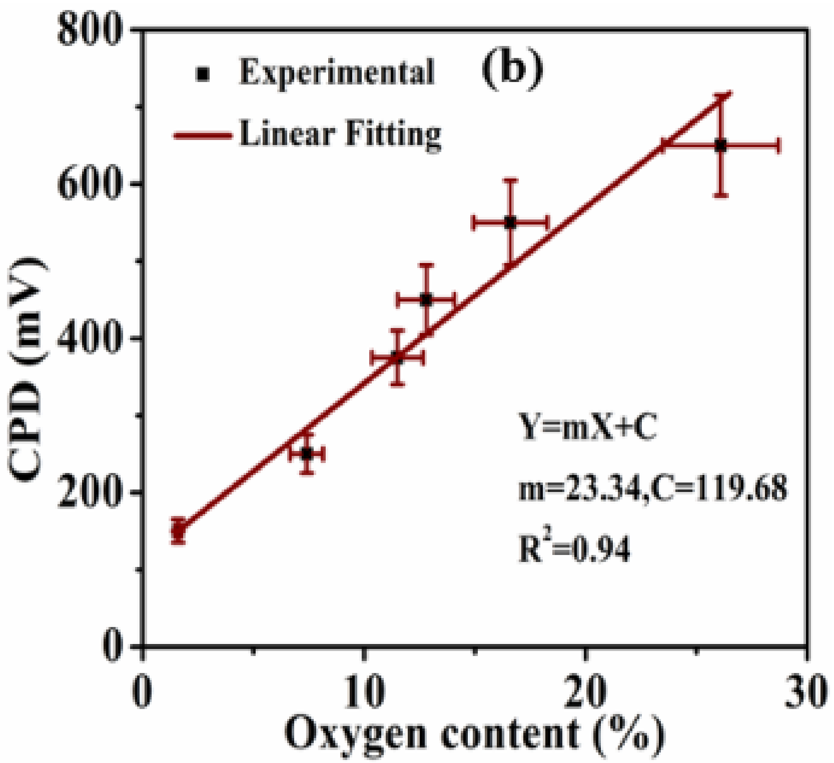

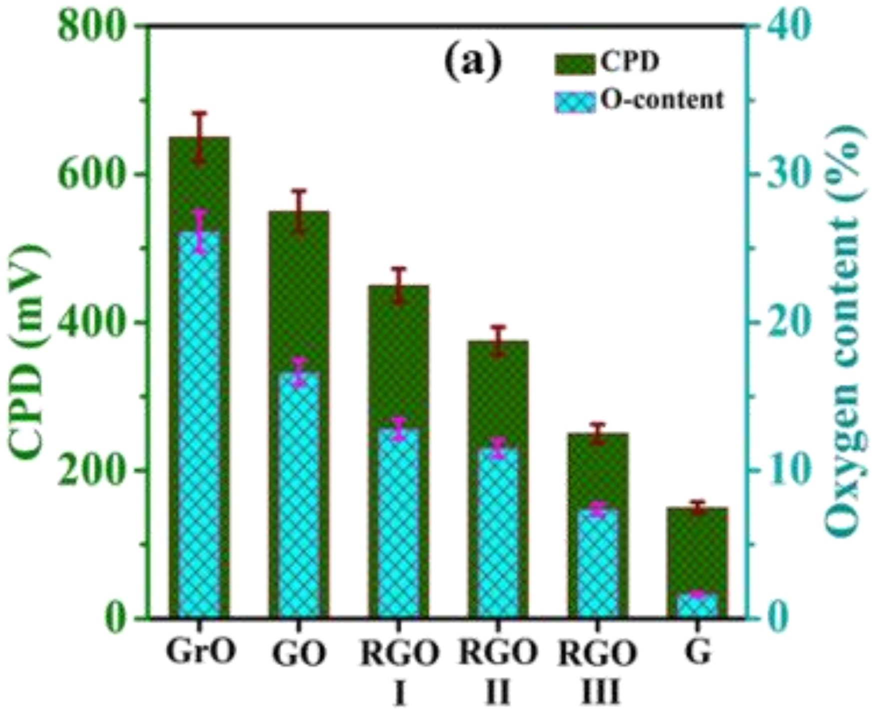

Relative surface contact potential difference (CPD) measurement between two different surfaces following the relation:

$$V_{\mathrm{CPD}} = \frac{(\Phi_{\mathrm{tip}} - \Phi_{\mathrm{sample}})}{e}$$

Here, Φ denotes work function, and e is the elementary charge of electron.

Using Au tip: $\Phi_{\mathrm{tip}} = 5.1$ eV

Mishra, Mukesh, et al. "Role of oxygen in the work function modification at various stages of chemically synthesized graphene." *The Journal of Physical Chemistry C* (2013).

Field effect transistor type gas sensors

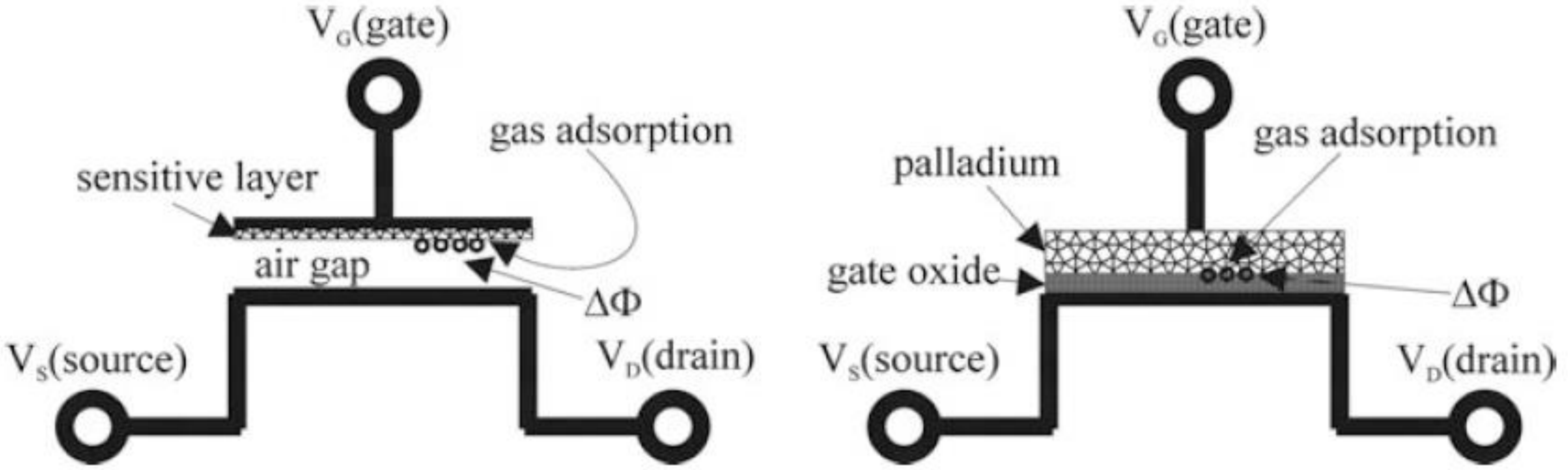

Fig. 2 Schematic view of an SG-FET (*left*) and a Lundström-FET (*right*)

Suspended gate field effect transistor gas sensors (SG-FET) belong to solid state gas sensors. In principle, they are capable of detecting a wide range of different gases by simply exchanging chemical-sensitive adsorption layers. This adsorption leads to a change in work function of the sensitive layer.

Fleischer, M., & Lehmann, M. (Eds.). (2012). Solid State Gas Sensors-Industrial Application (Vol. 11). Springer Science & Business Media.

Lundström-FET

Lundström developed the first gas sensor based on a conventional FET in 1975.

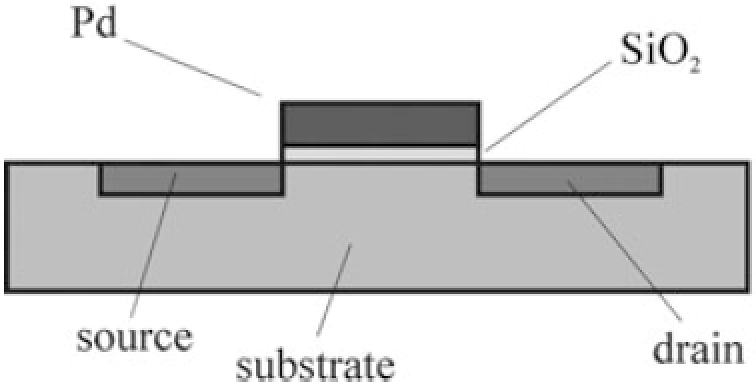

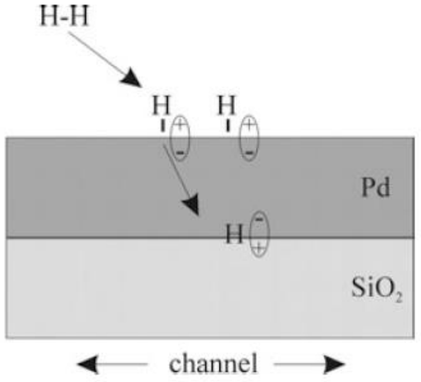

$$I_{DS} = \mu \frac{W_{\mathrm{eff}}}{L_{\mathrm{eff}}} C_I \left(V_G + \frac{\Delta\Phi}{e} - V_T \right) V_{DS}.$$

Here, μ denotes the carrier mobility; W_{eff} and L_{eff} are the effective channel dimensions of the transistor; e is the elementary charge; C_I is the oxide capacitance with respect to the area; and V_G and V_{DS} are the applied gate and source–drain voltages.

In summary. This FET has been proven to be a reliable sensor for hydrogen concentrations up to 1.5%.

Fleischer, M., & Lehmann, M. (Eds.). (2012). Solid State Gas Sensors-Industrial Application (Vol. 11). Springer Science & Business Media.

Lundström developed the first gas sensor based on a conventional FET in 1975.

Lundstrom discovered that when the gate was made of a thin layer of palladium, the atmospheric hydrogen would dissociate and diffuse through to the interface, creating a dipole layer and causing a shift in the threshold voltage. Using a circuit to drive a constant current through the device with common gate and drain terminals leads to a characteristic voltage response (equal to the shift in threshold voltage) of this type of device to hydrogen

$$\Delta V_{\mathrm{GDS}} = \Delta V_{\mathrm{T}} = \Delta V_{\max} \frac{k\sqrt{C_{\mathrm{H}}}}{1 + k\sqrt{C_{\mathrm{H}}}}$$

where **k** is a constant and **C_H** is the partial pressure of the hydrogen in air.
The solid palladium gate has subsequently been replaced by an ultrathin discontinuous metal film so that larger, less diffuse, molecules can reach the oxide surface and be sensed.

Gardner, Julian W., Vijay K. Varadan, and Osama O. Awadelkarim. *Microsensors, MEMS, and smart devices*. Vol. 1. New York: Wiley, 2001.

Suspended gate field effect transistor gas sensors (SG-FET)

In order to abolish the disadvantages of Lundstrom-type gas sensors, which come along with the essential need of a permeable gate material, an air gap between the sensitive layer and the gate oxide was introduced.

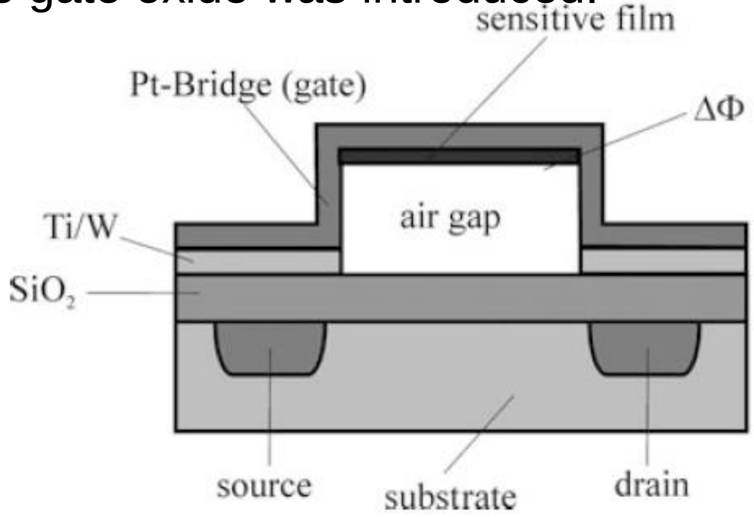

$$I_{DS} = \mu \frac{W_{eff}}{L_{eff}} C_{eff} \left(V_G + \frac{\Delta\Phi}{e} - V_T \right) V_{DS} \quad \text{with} \quad C_{eff} = \frac{C_I C_A}{C_I + C_A} . \qquad (2)$$

Here, C_I denotes the gate oxide capacitance, and C_A is the capacitance of the air gap and the sensitive layer. Because of the large air gap, C_A is very small in comparison to C_I, so $C_{eff} \approx C_A$. Consequently, the threshold voltage V_T is increased and can reach values up to 100 V.

Fleischer, M., & Lehmann, M. (Eds.). (2012). Solid State Gas Sensors-Industrial Application (Vol. 11). Springer Science & Business Media.

Suspended gate field effect transistor gas sensors (SG-FET)

تکنولوژی MEMS

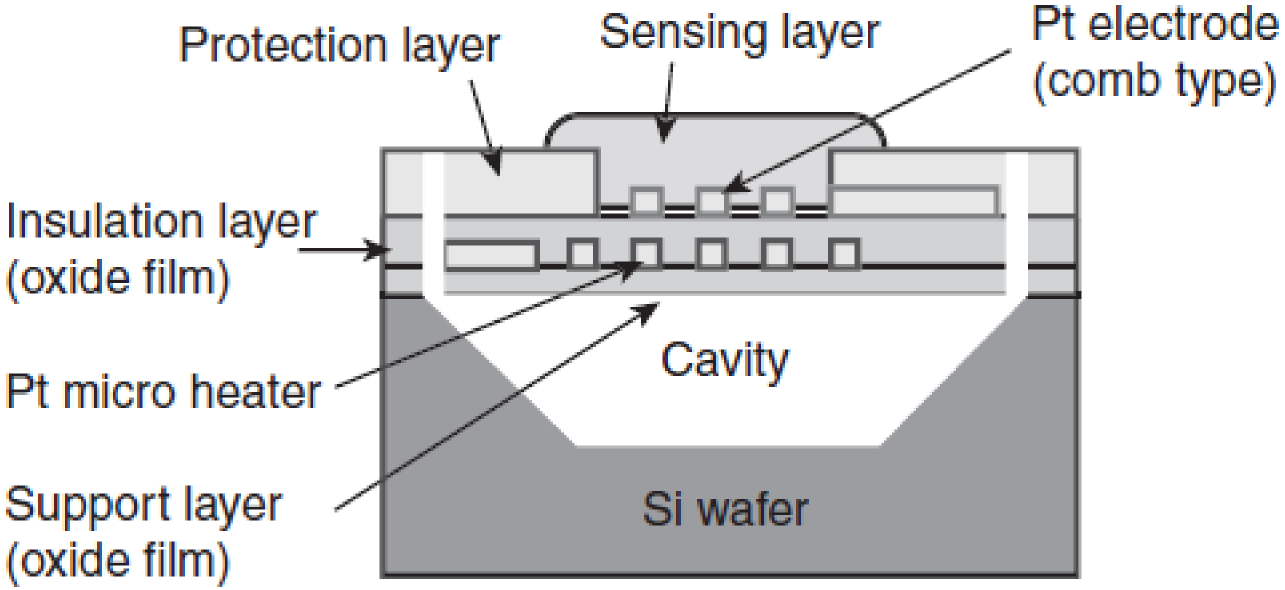

1.15 MEMS gas sensor.

Jaaniso, Raivo, and Ooi Kiang Tan, eds. Semiconductor gas sensors. Elsevier, 2013.

Field effect transistor type gas sensors

Pd-gate FET gas sensors

It responded to H2 and NH3 in air at 423 K. Reportedly, the H atoms dissociated from these molecules are dissolved into Pd metal and polarize in the vicinity of the border to the underlying insulator layer (SiO2) to modulate the electrical fild underneath.

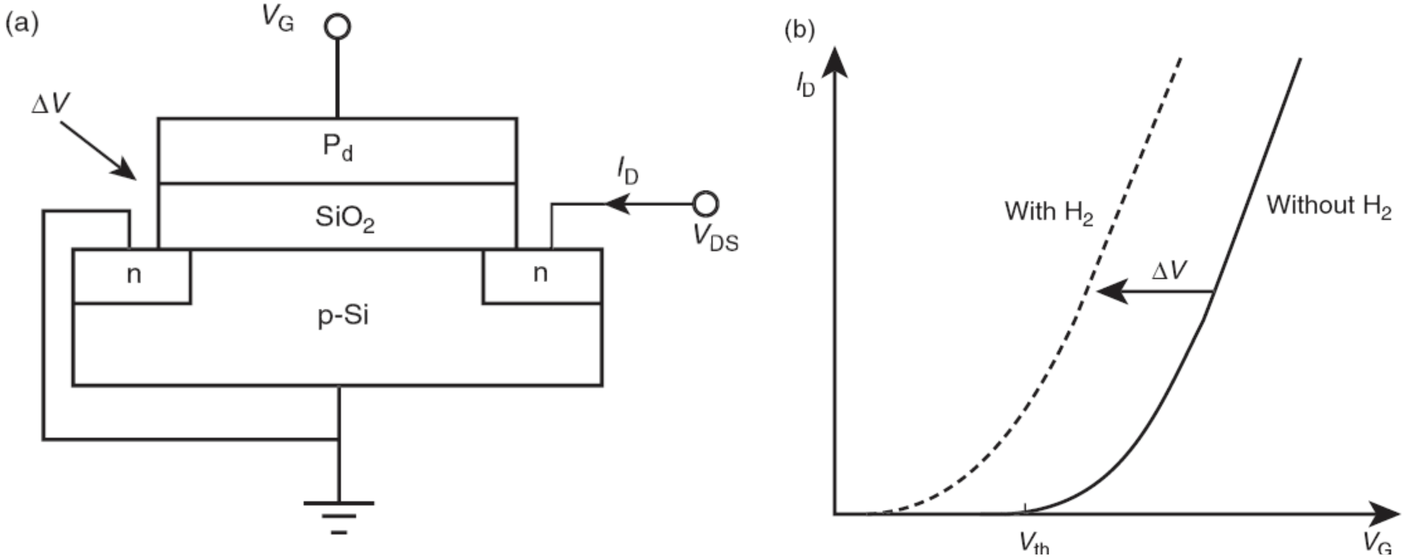

1.10 (a) Structure of Pd-gate FET. (b) Drain current (I_D) characteristics observed: V_G, gate voltage, V_{DS} (source–drain voltage).

Jaaniso, Raivo, and Ooi Kiang Tan, eds. Semiconductor gas sensors. Elsevier, 2013.

Field effect transistor type gas sensors

Solid electrolyte-gate field effect transistor

NO_2 sensor can be fabricated by attaching $NaNO_2$ (Na+ ionic conductor) and CO_2 sensor can be fabricated by Li_2CO_3 -based composite salt (Li+ ionic conductor) attaching to the gate metal.

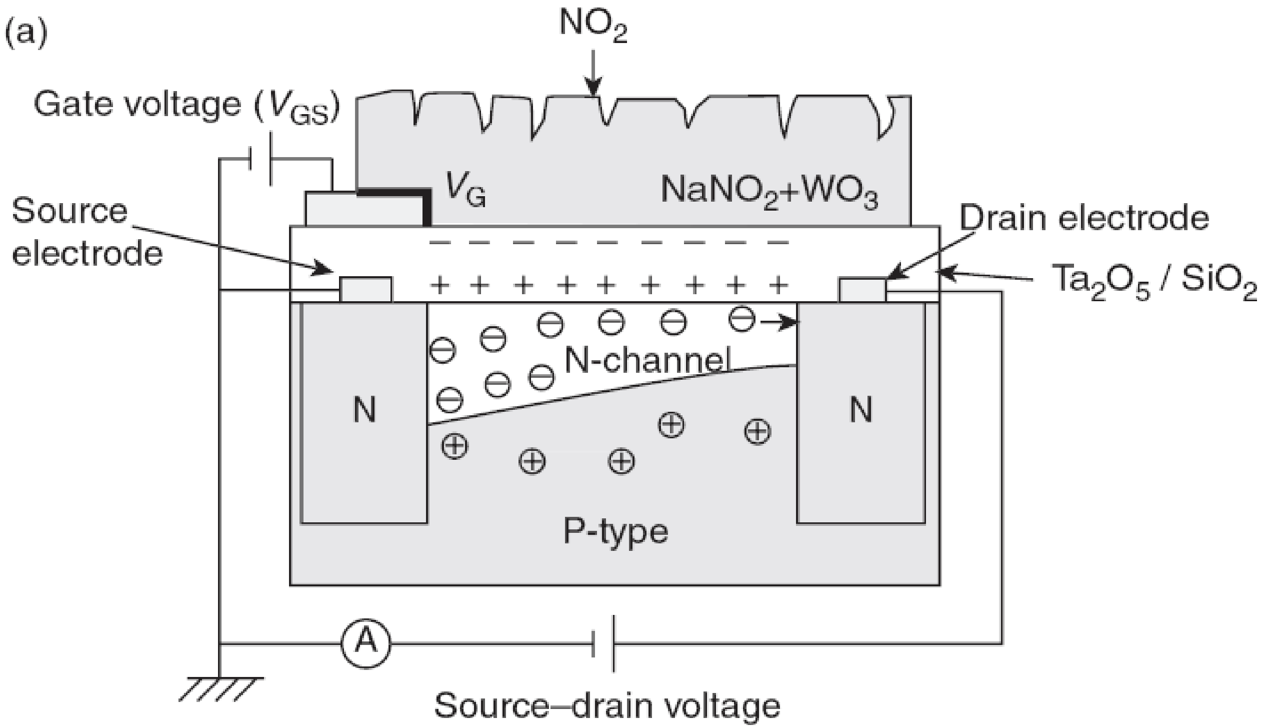

Construction of $NaNO_2$ -gate FET sensor.

Jaaniso, Raivo, and Ooi Kiang Tan, eds. Semiconductor gas sensors. Elsevier, 2013.

Field effect transistor type gas sensors

Solid electrolyte-gate field effect transistor

Three-phase contact between metal, solid electrolyte and gas is known to act as an active site for electrochemical reactions (half cell reaction).

$$NO_2 + e^- + Na^+ = NaNO_2,\ \Phi_M - \Phi_{SE} = \left(\frac{RT}{F}\right)\ln P_{NO_2} + \text{Constant}$$

The electrical potentials of metal and solid electrolyte are Φ_M and Φ_{SE}, respectively.

Φ_{SE} is raised higher than Φ_M , which is now controlled externally as gate voltage. This means that, at a fixed gate voltage, Φ_{SE} increases and, hence, the electrical field underneath also increases with increasing P_{NO2} .

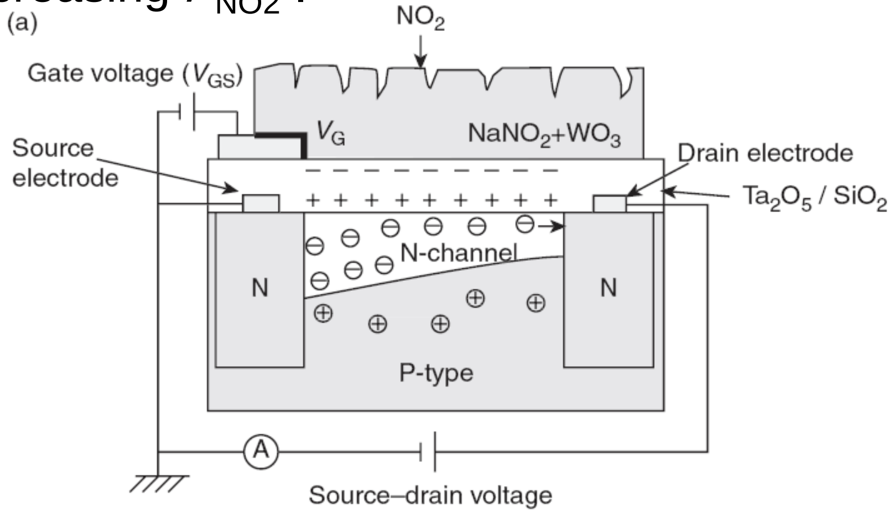

Field effect transistor type gas sensors

Oxide semiconductor-gate field effect transistor

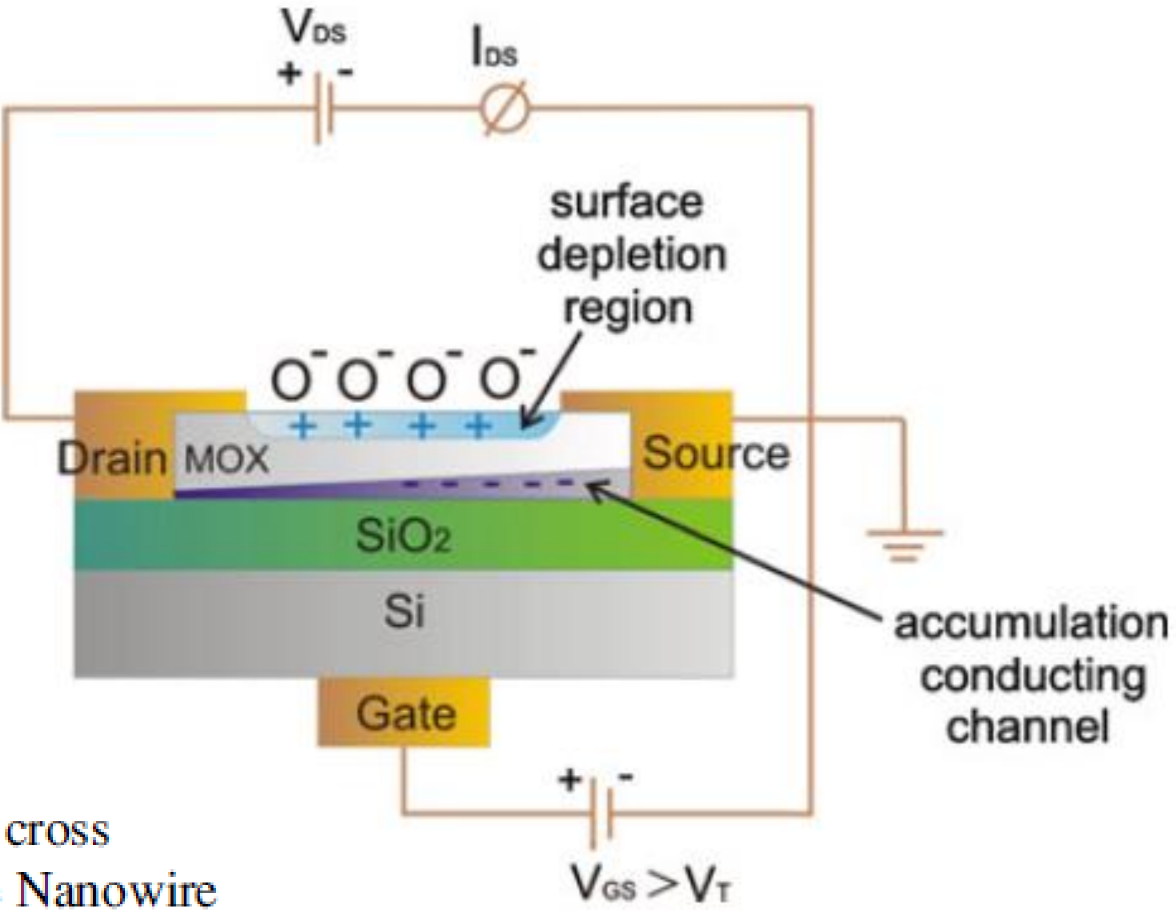

Fig. 8 Schematic cross section of a Single Nanowire n-type Transistor device in accumulation

Homola, Jirí, Marek Piliarik, and Róbert Horváth. "Springer Series on Chemical Sensors and Biosensors Methods and Applications." *Series Ed.: Wolfbeis, OS* (2006): 1612-7617.